Analysis of Mixed Formic and Acetic Acid Aggregates Interacting with Water. A Molecular Dynamics Simulation Study

Bastien Radola, Sylvain Picaud, Delphine Vardanega, Pal Jedlovszky

Analysis of Mixed Formic and Acetic Acid Aggregates Interacting With Water. A Molecular Dynamics Simulation Study

Bastien Radola[a], Sylvain Picaud[a,*],
Delphine Vardanega[a], Pál Jedlovszky[b,c]

[a]*Institut UTINAM - UMR 6213 CNRS, Univ. Bourgogne Franche-Comté, 16 route de Gray, F-25030 Besançon, France*

[b]*Department of Chemistry, Eszterházy Károly University, Leányka u. 6, H-3300 Eger, Hungary*

[c]*MTA-BME Research Group of Technical Analytical Chemistry, Szt. Gellért tér 4, H-1111 Budapest, Hungary*

Running title: Mixed formic and acetic acid aggregates interacting with water

*E-mail: sylvain.picaud@univ-fcomte.fr, phone: +33 3 81666478

Abstract:

Water adsorption on aggregates made of equimolar mixtures of formic and acetic acid molecules has been studied by means of molecular dynamics simulations between 150 and 275 K, covering thus a large range of atmospheric temperatures, as a function of both the water content and temperature. Calculations have shown that both the temperature and the water content have a strong influence on the behavior of the corresponding system. Two opposite situations have been evidenced for the acid – water aggregates at sufficiently high water content, namely water adsorption on large acid grains at low temperatures, and formation of a water droplet with an acid coating at high temperatures. In this latter case, acetic acid molecules have been found at the surface of the water droplet with their hydrophobic methyl group being as far as possible from the water surface, whereas part of the formic acid molecules were in the inner side of this interface. At low water content and high temperatures, this acid – water mixing was even more pronounced because the number of water molecules was not enough to completely dissociate the acid aggregate on which water molecules were adsorbed.

Comparison with previous simulations on water interacting with one component acid aggregates did not show any significant effect of the formic acid – acetic acid interactions on the behavior of the mixed systems. The results of the present simulations show how molecular scale approaches can help at better understanding the behavior of organic aerosols in the atmosphere. They also emphasize the need for further experiments and simulations to achieve a better characterization of the effects of temperature and humidity on the behavior of these aerosols.

1. Introduction

Atmospheric aerosols have an important, yet not well quantified role in defining the Earth's global climate on which they impact both directly by scattering and absorbing solar radiation, and indirectly, by acting as cloud condensation nuclei.[1,2] However, there is an increasing realization of the complexity of the aerosol composition, and, as a result, the uncertainty that affects their quantification has not been reduced decisively. It is even thought unlikely that in the near future it could be reduced in a way that would significantly improve our estimate of climate sensitivity.[3] This is especially true when considering the indirect effects of aerosols on the climate, which are even much less understood and quantified than the direct effects and, as a consequence, usually not taken into account in the climate models.[4] Indeed, the wide range of chemical and physical properties implied by the nature of the aerosols (inorganic vs. organic), their phase (solid vs. liquid), composition, mixing state, morphology, size and vertical distribution as well as their aging in the atmosphere hinders an easy characterization of the aerosol ability to nucleate ice particles and liquid droplets.[5] There is thus a need for better understanding the mechanisms underlying the interaction between aerosols and the surrounding water molecules. This would, however, require more detailed investigations, both from the experimental and the theoretical side, in a large temperature range typical of the atmospheric conditions from the boundary layer to the lower stratosphere.

Organic aerosols that contribute from 30 to 80 % of the total aerosol mass are one of the least understood components of atmospheric aerosols.[6] Although less hygroscopic than inorganic salts, ambient and laboratory-generated organic aerosols have been shown to absorb water depending on the particle size, composition, and also on the relative humidity.[7] Moreover, a handful of studies have shown the effect of the chemical composition on the physical state of atmospheric aerosols and the subsequent effect of this aerosol state on ice nucleation.[8-11] Indeed, at the low temperatures characteristic of the high troposphere and at low relative humidity, droplets containing a range of soluble organic compounds may become highly viscous or glassy. It has thus been suggested that many tropospheric organic aerosol particles are aqueous glassy solids.[12,13] However, the respective roles of glassy vs. liquid particles in cloud formation has only been a matter of speculation so far.[8]

Owing to the high complexity and variability of the organic aerosol phase, the modeling of simplified systems by computer simulations appears to be appealing as a first step toward a better understanding of the aerosol behavior, based on its description at the molecular scale. Thus, we recently conducted a set of studies, based on classical molecular dynamics (MD) simulations, to characterize the behavior of organic aggregates in contact with various amounts of water molecules at different temperatures.[14-17] We specifically focused on carboxylic acid species because they represent a significant part of the organic matter in the atmosphere.[18] In these studies, a classical rather than a quantum description of the intermolecular interaction between the molecules was used, because the modeling of realistic surrogates for the tropospheric aerosols requires to take into account hundreds of molecules in the calculations. Moreover, the use of such a classical approach was based on the confidence given by the successful comparison between the results of previous computer simulations of carboxylic acid molecules on ice and the corresponding experimental conclusions.[19-22] Thus, the behavior of the three smallest carboxylic (i.e., formic,[16] acetic and propionic[17]) and the two smallest dicarboxylic (i.e., oxalic,[14] malonic[15]) acid molecules has been characterized in detail in a broad range of temperatures and for different water:acid ratios.

The results showed that water and carboxylic acid molecules formed either mixed or demixed phases depending not only on the water:acid ratio and the temperature, but also on the type of the organic molecules. Moreover, these conclusions were in overall agreement with the results of other simulations based on a quite different approach, which characterizes the behavior of various organic molecules deposited on large water droplets.[23-28] More importantly, our results emphasized that the O:C ratio cannot simply be used as a proxy for characterizing the hydrophilicity of organic aerosols, as it has been suggested previously,[29] and that systematic experimental and/or theoretical studies involving a large series of organic molecules should be performed to definitely validate or invalidate the O:C criterion. Moreover, the situation can well be even more complex because of the likely influence of the morphology, physical state and composition of the aerosols on their behavior. We thus complement here our previous studies by the MD simulation-based characterization of the phase changes of large aerosol particles, formed by an equimolar mixture of formic and acetic acid molecules, when the temperature and the water content in the system are varied. Note that we have chosen these two acid molecules because they are among the most abundant organic acids in the atmosphere.[30]

The results essentially show that, for the systems simulated here, the behavior of mixed aerosol particles can be well predicted by knowing the behavior of the corresponding single acid particles studied separately. This conclusion thus supports recent models aiming at describing as simply as possible the hygroscopic and cloud condensation nucleation activity of complex multicomponent particles from the knowledge of their single-component counterparts.[31]

Our paper is organized as follows. The molecular dynamics simulations performed are detailed in Section 2 and the corresponding results are given in Section 3. The behavior of the systems under consideration is then discussed in Section 4. Finally, in Section 5, the most important conclusions of this study are summarized

2. Computational Details

The molecular dynamics simulations of formic (HCOOH) and acetic (CH_3COOH) acid aggregates interacting with water have been performed using the GROMACS 5.0.4 software package.[32] Simulations have been carried out on the canonical (*N,V,T*) ensemble with a time step of 1 fs. The Bussi thermostat, known as the velocity-rescaling thermostat in GROMACS, has been used with coupling times of 0.1 ps, offering the advantages of the standard Berendsen thermostat with the addition of a stochastic term allowing to model the correct thermodynamic ensemble.[33]

The atom-atom interaction potentials have been represented by sums of Lennard-Jones (6-12) and Coulomb terms. For acetic acid, force field parameters have been taken from the OPLS-AA library,[34] while the equilibrium geometry of the molecule has been determined using the Automated Topology Builder.[35] The model proposed by Jedlovszky and Turi[36] has been used to represent both the geometry and the interaction parameters of the formic acid molecules. Moreover, due to the large number of water molecules present in the simulation box when considering high water:acid ratios, water molecules have been represented by the four-site TIP4P/2005 model,[37] which offers a good reproduction of the properties of water in a broad range of thermodynamic states on a reasonably low computational cost, as compared with those of the five-site TIP5P model[38] used in our previous studies. The Lennard-Jones and electrostatics interactions were truncated with a cutoff distance of 1.4 nm. The Particle Mesh Ewald (PME) algorithm[39] has been used in order to properly take into account the long range part of the electrostatic interaction, with a relative tolerance of 10^{-5}, fourth-order cubic

interpolation, and a Fourier spacing parameter of 0.15 nm. All intra-molecular bonds have been kept rigid using the LINCS algorithm,[40] whereas no constraint has been applied on the internal angles of the molecules.

MD simulations have been performed using an aggregate made of an equimolar mixture of acetic and formic acid molecules. This aggregate has been created in the following way. First, 350-350 formic and acetic acid molecules have been continuously inserted into the large, cubic basic simulation box of the edge length of 10 nm during a 4 ns long initial simulation, performed at 150 K. This procedure has led to the formation of a single, compact aggregate of 700 molecules at the center of the simulation box. Then, a simulated annealing procedure has been performed by linearly heating the system up to 250 K during 2 ns, followed by a linear cooling down to 150 K in an additional 2 ns long run. Finally, a 10 ns long equilibration run has been performed, leading to the creation of a well-equilibrated and almost spherical aggregate in the simulation box (see below).

Then, five systems with different water contents have been built by randomly placing the required number of water molecules around the dry acid aggregate. These systems have corresponded to the water:acid ratio of 0:1, 1:1, 2:1, 4:1 and 8:1, the number of water molecules being thus varied from 0 to 5600. For each system simulated, water molecules have been progressively added in the box, each addition step being followed by a long equilibration run. This step required 40-100 ns long simulation runs depending on the water content. The equilibration of the systems has been checked by loocking at the energy stabilization and also by checking the stability of the radius of gyration of the particles formed in the simulation box.

The initial box edge length of 10 nm has also been increased up to 14 nm with increasing water content to accommodate all the water molecules in the basic box. Only protonated acid molecules have been considered in the simulations, as simple pK_A calculations show that less than 1 % of the acid molecules can be in the ionic form at the acid concentrations considered here. Note that this assumption agrees also well with the results of vibrational sum frequency generation spectroscopy measurements, which proved that acetic acid remains protonated in aqueous solutions in a large concentration range at 277 K.[41]

In order to characterize the influence of the temperature on the phase behavior of the acid – water aggregates, the various systems considered have progressively been heated by successive steps of 25 K, starting from the systems equilibrated at 150 K. During a 25 K step,

the temperature has linearly been increased first during a 1 ns long run, which was followed by a 9 ns-long equilibration run. Six temperature values have been considered, ranging from 150 to 275 K. Production runs of 2 ns have then been carried out for each temperature and water:acid ratio, leading to the detailed analysis of 30 simulation runs. It should be noted that, as in our previous studies, the temperature range considered here exceeds the one which can be encountered in the Earth's troposphere. However, it is important to note that the melting temperature of the TIP4P/2005 water model, used in the present study, is around 252 K,[37,42] i.e., about 20 K below the melting temperature of real I_h ice. Using this potential model thus certainly introduces a temperature shift when compared to the real systems,[42] the estimation of which being, however, very difficult when such a potential is used in combination with other models (such the acid models in the present study). Nevertheless, the large range of temperature values considered here allows shedding light to all the possible structural changes in the studied acid – water systems, as explained below.

3. Results

3.1. Structure of Neat Acid Aggregates

As described in Section 2, formic and acetic acid molecules were initially randomly scattered in the simulation box at 150 K, and the corresponding system has been equilibrated during a long simulation run. This led to the formation of a single, big aggregate of 700 molecules in the simulation box, as evidenced by the examination of several snapshots taken from the simulation (see top of Figure 1). Upon increasing the temperature from 150 to 275 K, this acid aggregate remained stable, as observed in previous simulations of one component aggregates of formic and acetic acid molecules.[16,17] Again, this has been evidenced by the examination of the equilibrium snapshots (top of Figure 1), and also supported by the statistical analysis of the structural characteristics of these aggregates through the calculations of the cluster size distributions $P_{acid}(n)$ in the simulation box, where the term 'cluster' refers to an ensemble of molecules linked together through hydrogen bonds. Criteria for bond lengths have been obtained using the first minimum position of the pair radial distribution functions of the relevant atomic pairs. Thus, two acid molecules have been considered as neighbors in the same cluster if the distance between the carboxylic hydrogen atom or any of the methyl hydrogen

atoms of one of these molecules and the oxygen atom of the other molecule was smaller than 0.225 or 0.350 nm, respectively. Then, in the whole temperature range considered here, $P_{acid}(n)$ showed only one single peak, for $n = 700$, indicating that all the formic and acetic acid molecules stayed packed together, irrespective of the temperature.

Note that the temperature range of the simulations would likely allow the formic and acetic acid molecules to be in the solid state. However, although density profiles and hydrogen bond distributions showed evidence for some local ordering (see Section 3.2), the aggregates simulated here have been characterized by a high surface to bulk ratio due to their relatively small size, and by an intricate mixing between the two acid species that prevented the formation of a well-ordered crystalline structure, even at 150 K.

3.2. Phase Behavior of Acid – Water Aggregates

Then, as detailed in Section 2, the influence of the amount of water molecules in the simulation box has been investigated for different water:acid ratios and temperatures. By looking first at the equilibrium snapshots (some of them being displayed in Figure 1), it can be clearly seen that the water molecules tend to form small clusters adsorbed at the surface of the acid aggregates at low temperatures, a situation that corresponds to a demixing of the acid and water phases. Of course, the higher the water content is, the larger is the surface of the acid aggregate covered by the water molecules (as evidenced by the snapshots given at the left hand side of Figure 1, from top to bottom). Upon increasing the temperature, water molecules penetrate into the acid aggregate, progressively dissolving it and pushing the acid molecules to the surface of the system. This behavior appears, in fact, to be very similar to what has been obtained from simulations of the formic acid – water[16] and the acetic acid – water[17] systems, previously simulated separately. Note that we have also performed some simulations by decreasing the temperature from 275 to 150 K. While the behavior of the dry acid aggregate appears reversible, i.e., it is very similar to the one observed when the temperature is increased, this is not the case for the mixed acid—water systems during the same simulation durations. Indeed, going from disorder to order is usually a difficult task in MD simulations, and the reversibility of the demixing processes obtained by decreasing the temperature would certainly need much longer simulations. We thus comment in the following only the results obtained when the temperature was increased.

Again, more insightful details can be extracted from the analysis of the cluster size distributions, $P(n)$. Thus, five cluster size distributions have been computed, namely, that of the clusters formed by acetic acid ($P_{ace}(n)$), formic acid ($P_{for}(n)$) or water molecules ($P_{w}(n)$) separately, by formic and acetic acid molecules, considered together ($P_{ace+for}(n)$), and by all the molecules in the simulation box ($P_{ace+for+w}(n)$). As above, these molecules have been considered as being in the same cluster if they have been linked to each other by hydrogen bonds, defined as the distance between their respective O and H atoms being smaller than the first minimum position of the corresponding radial distribution function. Thus, in addition to the criteria defined above for clustering of acid molecules, two water molecules have been considered as neighbors in the same cluster if the distance between a hydrogen atom of one of these two molecules and the oxygen atom of the other one was smaller than 0.225 nm. Similarly, a water molecule was considered to be the neighbor of an acid molecule if there was an O…H distance between the two molecules smaller than 0.225 nm, except for a bond involving a hydrogen atom of the acid methyl chain, for which the criterion was 0.375 nm.

Some of the corresponding $P(n)$ distributions are presented in Figure 2, as obtained at three different temperatures and three water:acid ratios (i.e., three different numbers of water molecules in the simulation box). Note that only a limited set of distributions is shown here; graphs exhibiting similar behavior are omitted for clarity. Similarly, the distributions $P_{ace+for+w}(n)$ are not presented in Figure 2, since they all showed only one single peak at the value equal to the total number of molecules in the simulation box, indicating that there is always only one single, big aggregate, in the simulation box, irrespective of both the temperature and the water content.

At low temperature (150 K) and low water content (1:1 and 2:1 water:acid ratios; see Figure 2, upper and middle left panels), $P_{ace+for}(n)$ exhibits a quite narrow peak located near the $n = 700$ value, indicating that the vast majority of the 350 formic and 350 acetic acid molecules were linked together to form a large aggregate in the simulation box. Similarly, the cluster size distribution $P_{w}(n)$ for $N_{w} = 700$ and $N_{w} = 1400$ (N_{w} being the number of water molecules in the basic box) is also characterized by a narrow peak near the value of $n = N_{w}$ indicating that no isolated water molecules can be found in the simulation box. Interestingly, while the $P_{ace}(n)$ distribution shows that almost all the acetic acid molecules are linked together, as indicated by the distribution peak around the value of $n = 300$, it turns out that the size of the formic acid

clusters is significantly smaller than the maximum of 350, and thus a significant number of formic acid molecules are isolated from the other formic acid molecules in the box (as indicated by the significant intensity of the peak at $n = 1$ in $P_{for}(n)$). These features could be explained by a stronger mixing of the formic than the acetic acid molecules within the acid aggregate. The increase of the temperature leads to a general shift of the peaks of the $P_{for}(n)$ and $P_{ace}(n)$ distributions to lower n values, this shift being even more pronounced for the formic than for the acetic acid molecules. However, the $P_{ace+for}(n)$ distribution still exhibits a large, single, peak near the value of $n = 700$, even at the highest temperature of 275 K considered here. This clearly indicates that there is a large acid aggregate in the simulation box, irrespective of the temperature, which is characterized by an increasing mixing between formic and acetic acid species upon temperature rise. Meanwhile, $P_w(n)$ shows a slight shift toward smaller n values with increasing temperature due to the larger thermal motion of the molecules. These results are consistent with the behavior of a system initially made of an acid aggregate covered by water molecules, which is then characterized by the penetration of some water molecules more and more deeply in the core of the acid aggregate when the temperature is increased. However, when acid and water molecules are in a 1:1 or 2:1 ratios, a complete dissolution of the acid cluster in water has not been observed.

By contrast, at very high water content (8:1 water:acid ratio), the increase of the temperature finally led to the complete dissolution of the acid aggregate, as shown by the single peaks obtained at $n = 1$ in the various cluster distributions related to the acid molecules at 275 K (bottom of Figure 2). Moreover, the large peak around $n = 5600$ in $P_w(n)$ indicates the presence of a very large water droplet in the simulation box. These results fully support the conclusions drawn from the examination of the snapshots, i.e., that high water content and high temperature are responsible for the complete dissolution of the acid aggregate, and the formation of a large water droplet.

Note that because the $P(n)$ distributions may be sensitive to the criteria used to find the next neighbors, we have modified the distance criteria by up to ± 0.05 nm in order to characterize the influence of this choice on the results. However, no fundamental difference has been evidenced in the results, giving confidence in the conclusions drawn above.

In addition to the $P(n)$ curves, the results on cluster size distributions can be described in a more compact way by the calculation of the average size of the acid aggregates all along the simulations, using the following equation :

$$\overline{n_x} = \langle \frac{1}{N_x} \sum_{n=1}^{N_x} n^2 P_x(n) \rangle_t \quad (1)$$

where $\overline{n_x}$ is the average size of clusters composed of molecules of type X (i.e., formic or acetic acid), N_x is the total number of these molecules, n is the size of a cluster, and $P_x(n)$ is the number of molecules of type X being in clusters of size n, and the symbol $\langle ... \rangle_t$ denotes time average along the simulation trajectory. That way, the evolution of the structural characteristics of the aggregates as a function of temperature and water content can be easily observed and thus analyzed.

The corresponding curves for formic and acetic acid species, analyzed separately, are given in Figures 3a and 3b, respectively. They exhibit a similar behavior, showing that in the absence of water, the average formic acid and the average acetic acid cluster sizes remained almost constant, irrespective of the temperature. In contrast, the presence of water molecules in the simulation box led to the decrease of the average acid cluster sizes when the temperature has been increased. Above 225 and 250 K for the formic and acetic acid molecules, respectively, the average cluster size tended towards very small values, indicating that acid molecules of the same species are almost completely separated from each other, with the exception of the systems corresponding to 1:1 water:acid ratio, for which the average acetic acid cluster size resulted in a value corresponding to about 50 molecules at 275 K. This indicates that, at low water content, some clustering was still present between acetic acid molecules even at high temperature. Note that these results are very similar to those previously obtained for the two acid species simulated separately.[16,17]

Density profiles $\rho(r)$ have also been computed to get more information about the relative arrangement of acid and water molecules within the aggregates formed in the box during the simulation runs. Five different species or atomic groups were selected for analysis, namely formic acid ($\rho_{for}(r)$), acetic acid ($\rho_{ace}(r)$), water ($\rho_{w}(r)$), as well as the methyl ($\rho_{meth}(r)$)

and carbonyl ($\rho_{carb}(r)$) groups of acetic acid. These density profiles are related to the positions of the center-of-mass of the selected molecules or atomic groups, with respect to the position of the center-of-mass of the aggregate in the simulation box.

Some of these density profiles $\rho(r)$ are presented in Figures 4a and 4b. Note that although these density profiles may present large oscillations at low r values because of the poor statistics on small spherical volumes, $\rho_{ace}(r)$ and $\rho_{for}(r)$ also exhibit several real peaks at low temperature values, typically up to 175 K, irrespective of the water content. These peaks can be related to the formation of a partially crystallized acid aggregate, at the surface of which water molecules are adsorbed, as indicated by the position of the broad peak of $\rho_w(r)$ at large r values (left column in Figure 4a). In contrast, at 275 K, $\rho_w(r)$ exhibits an almost constant value in a large range of r values, which is typical of the formation of a disordered water droplet in the simulation box (right column of Figure 4a). Morever, the density profiles indicate that this droplet contains a lot of acid molecules at low water:acid ratio. The behavior of $\rho_w(r)$ at intermediate temperature (typically between 200 and 250 K) evidences the progressive penetration of the water molecules into the acid aggregate initially formed in the simulation box (middle column of Figure 4a). Meanwhile, a large fraction of the acid molecules are pushed to the surface of the water droplet as the temperature is increased, as shown by the peaks observed in $\rho_{ace}(r)$ and $\rho_{for}(r)$ curves at large r values corresponding to the location of the droplet surface. However, the long tail of $\rho_{ace}(r)$ and $\rho_{for}(r)$ at small r values and intermediate temperatures indicates that part of the acid molecules may remain in the aqueous phase, the ratio of the bulk and surface acid molecules decreases with increasing water content, and it is higher for formic than for acetic acid.

In addition, the analysis of $\rho_{meth}(r)$ and $\rho_{carb}(r)$ (Figure 4b) shows that the peak corresponding to the preferred location of the carboxylic groups is always closer to the aggregate center than that of the methyl group, indicating that the acetic acid molecules are oriented with their methyl groups away from the water molecules, as expected from simple chemical considerations. The presence of this hydrophobic tail may, of course, explain the different behavior of acetic and formic acids with respect to the water droplet formed during the course of the simulations. Note that for the formic acid molecules located at the interface, the analysis of the density profiles calculated separately for the H atoms and the COOH groups

(not shown) also indicate a preferential adsorption with the carboxyl group oriented toward the droplet side of the interface.

Overall, these results are fully consistent with those previously obtained with formic acid/water and acetic acid/water systems simulated separately,[16,17] where formic acid molecules were found to mix with water even at high temperatures and high water content, whereas acetic acid molecules formed fully separated phases in these conditions.

3.3. Energetic Background

In order to have a better understanding of the energetic background laying behind the structural changes inside the aggregates upon increasing the temperature and/or the water content, various binding energy distributions $P_{X–Y}(E_b)$ have been computed, where X and Y stands either for formic acid (X or Y = for), acetic acid (X or Y = ace), or water (X or Y = w) molecules. The distributions have been calculated with respect to molecule X, i.e., they represent the binding energy distribution of one molecule of species X with all molecules of species Y in the simulation box.

A selection of these binding distribution energy curves is given in Figure 5a for the interaction involving only acid molecules, and in Figure 5b for the interactions involving water molecules. At low temperature, it can be seen that the energetic behavior of the acid – water systems does not depend strongly on the water content. For instance, at 150 K, three peaks are obtained for $P_{w–w}(E_b)$ at about -110 kJ/mol, -80 kJ/mol and -60 kJ/mol, irrespective of the water content, although the intensity of these peaks may change upon addition of water molecules in the simulation box. Considering that the energy of a hydrogen bond between two water molecules is around -27.5 kJ/mol with the TIP4P/2005 interaction potential,[37] $P_{w–w}(E_b)$ curves indicate that the water molecules form two to four hydrogen bonds with other waters in the systems simulated here. Similarly, the energy distributions corresponding to the acid – acid (Figure 5a) and acid – water (Figure 5b) interactions are characterized by several broad peaks that do not depend on the water content at low temperature and that come from the formation of several hydrogen bonds between these molecules. The most interesting feature is certainly the large peak seen around zero energy in the $P_{for–w}(E_b)$ and $P_{ace–w}(E_b)$ acid – water energy

distributions, which can be related to a large amount of acid molecules that are completely separated from water molecules and do not noticeably interact with them. Therefore, the energetic results obtained at low temperature are in accordance with the conclusions drawn previously from the structural analysis, i.e., that the simulation box contains a large aggregate of acid molecules, at the surface of which water molecules form adsorbed clusters, irrespective of the water content.

Upon increasing the temperature, acid – acid and acid – water binding energy distributions change in the opposite way, the former one being shifted to higher, while the latter one to lower energy values. These two features clearly evidence the increase of the interaction between acid and water molecules at the expense of the acid-acid interactions, a tendency that is even stronger at high water content. Thus, at 275 K, the peak at 0 kJ/mol in $P_{\text{for–w}}(E_b)$ and $P_{\text{ace–w}}(E_b)$ has almost completely vanished, while the intensity of the peak at zero energy strongly increases in $P_{\text{for–for}}(E_b)$, $P_{\text{ace–ace}}(E_b)$, $P_{\text{for–ace}}(E_b)$ and $P_{\text{ace–for}}(E_b)$.

To complete this analysis, hydrogen bond distributions $P_{\text{X–Y}}(N_{\text{HB}})$ have also been computed by considering that two molecules X and Y are hydrogen bonded if the distance between two of their oxygen atoms is less than 0.35 nm, (i.e., the first minimum of the radial distribution function between O atoms) and, at the same time, the O…H distance is smaller than the first minimum position of the radial distribution between O and H atoms (i.e., 0.225 nm). Note that we used here the definition of H-bonds based on the physically relevant distances between O and H atoms instead of the definition based on the combination of the O…O distance and the O--H…O angle criteria (a H-bond is formed if this distance is less than 0.35 nm and this angle is less than arbitrarily chosen value, usually 30°). Thus, $P_{\text{X–Y}}(N_{\text{HB}})$ corresponds to the distribution of the number of hydrogen bonds formed between one molecule X with all the Y molecules present in the simulation box. Some of these distributions are shown in Figure 6, using the same color coding as in Figure 5. It can clearly be seen that, at low temperature, water molecules form two to four hydrogen bonds with their water neighbors, and this number increases with increasing water content (Figure 6b), in agreement with the conclusions drawn from the analysis of the corresponding binding energy distribution, given in Figure 5b. By contrast, the number of H-bonds formed between acid molecules (Figure 6a) and between acid and water molecules (Figure 6b) at low temperature remains similar, irrespective

of the water content. This, again, supports the results of the analysis of the binding energy distributions made above.

At higher temperature, a clear increase of the number of acid – water hydrogen bonds is evidenced in Figure 6b by a diminution of the peak at $N_{HB} = 0$ and the concomitant increase of the peak for the values of $N_{HB} = 1$ and 2 in $P_{ace–w}(N_{HB})$ and $P_{for–w}(N_{HB})$, at the expense of the number of acid – acid (Figure 6a) hydrogen bonds. Meanwhile, there is a clear increase of the number of water molecules that have four H-bonds with the increase of the water amount (Figure 6b). These features are again in accordance with the analysis of the energy distribution curves. However, two somehow different situations emerge from a more detailed analysis of the $P_{XY}(N_{HB})$ distributions. Indeed, at low water content, the probability of having still at least one hydrogen bond between acid molecules remains quite high, as seen from the $P_{ace–ace}(N_{HB})$, $P_{ace–for}(N_{HB})$, $P_{for–for}(N_{HB})$ and $P_{for–ace}(N_{HB})$ curves. On the other hand, at high water content the number of H-bonds formed between acid molecules is practically zero. Meanwhile, the $P_{ace–w}(N_{HB})$ and $P_{for–w}(N_{HB})$ distributions have their maximum at $N_{HB} = 1$ and $N_{HB} = 2$ at low and high water content, respectively. This is in accordance with the formation of a demixed phase, in which acid molecules are adsorbed at the surface of a large water droplet at high water content, and with some remaining acid – water mixing at lower water content.

In addition, differences between the intensities of the various peaks in $P_{ace–w}(E_b)$ and $P_{for-w}(E_b)$ distributions (Figure 6b) indicate that the behavior of the two acid species is not strictly equivalent. Indeed, acetic acid tends to form a slightly smaller number of hydrogen bonds with water than formic acid, at least at high temperature, supporting again that formic acid mixes somewhat better with water than acetic acid.

In summary, the analysis of both the hydrogen bond and the binding energy distributions at high water content supports the existence of a transition from a demixed phase, in which an acid aggregate is surrounded by water molecules at low temperature, to another demixed phase at higher temperature corresponding to the formation of a water droplet that adsorbs the majority of the acid molecules at its surface, with the exception of a small amount of formic acid that still remains mixed in the bulk of this droplet. In contrast, at low water content, this second demixed phase is never observed even at the highest temperature considered here. Instead, the majority of the acid molecules remain mixed with water, forming a mixed aggregate at the surface of which some acetic acid molecules can be found.

4. Discussion

The present simulation results have evidenced that the behavior of mixed formic and acetic acid aggregates interacting with different amounts of water molecules in a large temperature range could easily be derived from the behavior of each acid species interacting separately with water. As a consequence, the lack of any noticeable influence of the formic acid – acetic acid interactions on the behavior of the system leads to conclusions similar to those obtained in our previous studies devoted to the pure formic[16] and acetic acid[17] aggregates. They are thus reinforced by the tests performed previously, and which have shown that the results do not dramatically depend on the models used to describe the interactions between water molecules, and that the duration of the simulations was sufficiently long to ensure good equilibration of the systems under investigation. Similarly, the present conclusions may also suffer from the same lack of direct comparison with any experimental studies performed under similar conditions. Indeed, to the best of our knowledge, there is only one experimental study that has been devoted to the characterization of acetic acid and formic acid aerosols mixed with water molecules by infrared spectroscopy.[43] Moreover, the comparison of the results of this study with our results could only be qualitative, because the temperature of the experiments (78 K) was much lower, and the size of the aggregates much larger (10 to 600 nm) than the ones considered here. Moreover, the two acids were characterized separately in the experiments. Nevertheless, these experimental results showed that both pure acetic acid and pure formic acid particles exhibit a partial crystal form at low temperature, and that this crystalline structure disappears when adding a certain amount of water molecules. In addition, formic and acetic acids were shown to behave differently when adding water, formic acid absorption bands being more sensitive to the composition than those of acetic acid in the acid/water mixtures. This feature was related to a better mixing between formic acid and water than between acetic acid and water molecules, in accordance with the results of the present study, and also, with those of our previous studies.[16,17]

Moreover, vibrational sum frequency generation spectroscopy (SFG) experiments, aiming at characterizing the liquid-gas interface of acetic acid – water mixtures at 277 K[41,44] have shown that even a small amount of acetic acid may disrupt the water surface significantly. The orientation of the interfacial acetic acid molecules was found to be perpendicular to the

interface, with the methyl group directed toward the gas phase, irrespective of the acid concentration, again in accordance with our present findings. In addition, it has been recently shown that the average number of hydrogen bonds formed by fully hydrated acetic acid molecules is about 2.5.[45] This number is significantly higher than what is calculated here (see Figure 6b), and thus reinforces our findings that acetic acid molecules prefer to stay at the surface rather than inside the bulk of the water droplet, being thus not fully hydrated at high temperature and high water content. The present conclusions are also in agreement with the results of X-ray photoelectron spectroscopy (XPS) experiments that have shown evidence for high carboxylic acid concentrations at aqueous solution-air interfaces and for the carboxyl group pointing preferentially toward the bulk (aqueous) side of the interfacial region.[46,47]

The ability of the aggregates simulated here to act as nuclei for further water condensation at tropospheric temperatures should also be discussed, at least qualitatively. At these temperatures, our results show that formic and acetic acid molecules form stable aggregates, on which water molecules can be adsorbed. However, upon increasing the water amount around the aggregates (which can be related to an increase of the relative humidity), the dissolution of the acid aggregate is observed, with the concomitant aggregation of the water molecules and the migration of the acid molecules to the subsurface (formic acid molecules) and surface (acetic acid molecules) region of the resulting water aggregate. The gas/particle interface of the water/acid systems is thus made of a mixture of water and acid molecules, which can impact on the subsequent growth of the particle, depending on the probability that an incoming water molecule interacts with a surface water (strongly attractive interaction) or with a surface acid molecule (weaker interaction). In the systems simulated here, simple geometric considerations taking into account both the size of the water droplet formed in the simulation box and the projected area of an acetic acid molecule standing upright at the water surface show that at 275 K the maximum amount of the acetic acid molecules located at the surface covers around 40 % of the surface droplet for systems containing moderate amounts of water, and decreases down to 25 % when adding more water molecules in the system (8:1 water:acid ratio). These non-negligible proportions indicate that the value of the sticking coefficient of incoming water molecules on such aggregates may noticeably differ from 1 (i.e., from the sticking coefficient of water molecules onto water, as calculated from molecular dynamics simulations)[48]. Unfortunately, experimental measurements of such coefficient are challenging

and, as recently stated, the measured value may vary by orders of magnitude depending on the experimental technique used, even for pure water.[49]

As stated in the Introduction part of the paper, it has been suggested that many tropospheric organic aerosol particles could be aqueous glassy solids.[12,13] In MD simulations, a suitable probe for the characterization of such glassy states and phase transitions from glassy to liquid states is the time autocorrelation function (ACF) of the angle formed by the position vectors of a pair of atoms within each molecule under investigation.[50,51] Indeed, if ACF approaches a constant value well above zero, this indicates a rather frozen system whose internal structure evolves too slowly for ACF angle to drop to zero, in contrast to liquid-like systems for which this ACF would rapidly vanish. We have thus calculated the ACF for the angles formed by two H atoms located as far as possible from each other in formic and acetic acid molecules, at the lowest (150 K) and the highest (275 K) temperatures considered here and for a 2:1 water:acid ratio, as an example. The corresponding curves, given in Figure 7, clearly exhibit glassy-like and liquid-like behaviors for the acid molecules at 150 and 275 K, respectively. Moreover, the shape of these curves indicates that the dynamics of the acid molecules could be characterized by different time scales, which can be analyzed from a fit of the ACF curves by exponential or biexponential forms, as suggested by previous studies on glassy systems[50,51]. Unfortunately, while such fits seems to give reasonable results for the dynamics of acetic acid molecule, they are less satisfactory for the formic acid molecules, a feature that could be related to the remaining mixing of these molecules in water, even at high temperature. We thus concluded that the full detailed investigation of the internal dynamics of the systems considered here could be a difficult task, appearing to be far from the scope of the present paper which is mainly focused on the structure of the mixed organic acid aggregates in contact with water. This problem, however, deserves further investigations, which have to be first performed on separate acid systems in water before to be extended to mixed acid aggregates.

Finally, it is worth noting that recent experimental investigations devoted to the characterization of the behavior of various secondary organic aerosols under the influence of increasing level of relative humidity (RH) have evidenced the occurrence of a semisolid-to-liquid phase transition at elevated RH, the RH threshold for this transition varying with the nature of the organic molecule considered (i.e., isoprene, α-pinene, and toluene).[52] More

importantly, it was also shown that the absorbed water volume is a dominant governing factor for the semisolid-to-liquid phase transition and, as a general conclusion, it was finally stated that both the chemical composition and the RH influenced the phase state of organic particles.[48] This conclusion is in nice agreement with the behaviors evidenced for acid organic aerosols, not only here but also in our previous simulation studies.[14-17]

5. Conclusions

Molecular dynamics simulations have been used to characterize, at the molecular level, the interaction between organic aerosols and the surrounding water molecules as a function of the temperature and the water content. The organic aerosols have been modeled by a mixture of formic and acetic acid molecules to account for the influence of the aerosol composition in its phase behavior at various levels of humidity. Different situations have emerged from the simulations performed under different conditions. At low temperature, a demixed phase has been obtained, in which clusters of water molecules are formed at the surface of a more or less structured organic aerosol, made of a mixture of formic and acetic acid molecules, irrespective of the number of water molecules in the simulation box. At higher temperatures, two different behaviors have been evidenced, depending on the water:acid ratio. At high water content, a complete dissolution of the organic aggregate has been achieved and the formation of a big water droplet has been observed in the simulation box, on which acid molecules are adsorbed, forming a new demixed phase. In this phase, acetic acid molecules are located at the surface of the droplet, with their methyl group oriented toward the gas phase, whereas most of the formic acid molecules prefer to stay in the subsurface region of the droplet. By contrast, at high temperature and low water content, formic acid and water molecules have shown a tendency to form a mixed aggregate, at the surface of which part of the acetic acid molecules are adsorbed.

The phase changes evidenced by the simulations could be of particular interest for atmospheric models, because they show that the aerosol-gas interface may depend not only on the temperature and humidity, but also on the composition of the organic aerosol. In particular, in conditions that favor the hydrophobic groups of the organic species being at the surface, a potential inhibition of the propensity of aerosols to act as cloud condensation nuclei should be taken into account.

Moreover, the present conclusions on the phase changes observed for the acid aggregates upon the increase of the water content as well as the temperature could be of importance with respect to the problem of the oxidation-transformation of the organic molecules in the Troposphere, given the accessible-inaccessible character of this organic matter in the mixed acid-water aggregates at different temperatures and relative humidities.[53-55] Indeed, our results clearly show that, under certain conditions, some organic acid molecules adsorbed at the surface of the aerosol particle may be quite easily attacked by oxidizing agents, while part of these acid molecules remain protected, being buried in the aqueous phase. Simulations at the molecular scale can thus help understanding the key physical properties (phase, viscosity, morphology, etc.) of ambient aerosols particles that may influence the rates, products, and impacts of heterogeneous oxidation under a range of atmospheric conditions.

Finally, the present results clearly show that the behavior of a binary aggregate of small carboxylic acid molecules, such as formic and acetic acids, interacting with water may be directly derived from the behavior of the corresponding single species aggregates. This conclusion could support the idea that the representation of hygroscopic growth and cloud condensation activity of multicomponent particles can be derived from the known properties of their individual constituents.[31]

Acknowledgements

This project has been supported by the Hungarian-French Intergovernmental Science and Technology Program (BALATON) under project No. TéT_15_FR-1-2016-0056, by the Hungarian NKFIH Foundation under project No. 119732, and by the Observatoire OSU THETA of Besançon. Simulations have been performed thanks to the computing resources of the Mésocentre de Calcul, a Regional Computing Center at Université de Franche-Comté.

References

(1) Satheesh, S.K.; Krishna Moorthy, K. Radiative Effects of Natural Aerosols: A Review. *Atmos. Environ.* **2005**, *39*, 2089-2110.

(2) Lohmann, U.; Feichter, J. Global Indirect Aerosol Effects: A Review. *Atmos. Chem. Phys.* **2005**, *5*, 715-737.

(3) Le Treut, H. Greenhouse Gases, Aerosols and Reducing Future Climate Uncertainties. *Surv. Geophys.* **2012**, *33*, 723-731.

(4) Levy II, H.; Horowitz, L.W.; Schwarzkopf, D.; Ming, Y.; Golaz J.C.; Naik, V.; Ramaswamy, V. The Roles of Aerosol Direct and Indirect Effects in Past and Future Climate Change. *J. Geophys. Res. Atm.* **2013**, *118*, 4521-4532.

(5) Shiraiwa, M.; Zuend, A.; Bertram, A.K.; Seinfeld, J.H. Gas-Particle Partitioning of Atmospheric Aerosols: Interplay of Physical State, Non-Ideal Mixing and Morphology. *Phys. Chem. Chem. Phys.* **2013**, *15*, 11441-11453.

(6) Hallquist, M.; Wenger, J.C.; Baltensperger, U.; Rudich, Y.; Simpson, D.; Claeys, M.; Dommen, J.; Donahue, N.M.; George, C.; Goldstein, A.H.; et al. The Formation, Properties and Impact of Secondary Organic Aerosol: Current and Emerging Issues. *Atmos. Chem. Phys.* **2009**, *9*, 5155-5236.

(7) Jathar, S.H.; Mahmud, A.; Barsanti, K.C.; Asher, W.E.; Pankow, J.F.; Kleeman, M.J. Water Uptake by Organic Aerosol and its Influence on Gas/Particle Partitioning of Secondary Organic Aerosol in the United States. *Atmos. Environ.* **2016**, *129*, 142-154.

(8) Murray, B.J.; Wilson, T.W.; Dobbie, S.; Cui, Z.; Al-Jamur; S.M.R.K.; Möhler, O.; Schnaiter, M.; Wagner, R.; Benz, S.; Niemand, M.; et al. Heterogeneous Nucleation of Ice Particles on Glassy Aerosols Under Cirrus Conditions. *Nat. Geosci.* **2010**, *3*, 233-237.

(9) Wilson, T.W.; Murray, B.J.; Wagner, R.; Möhler, O.; Saathoff, H.; Schnaiter, M.; Skrotzki, J.; Price, H.C.; Malkin, T.L.; Dobbie, S.; et al. Glassy Aerosols With a Range of Compositions Nucleate Ice Heterogeneously at Cirrus Temperatures. *Atmos. Chem. Phys.* **2012**, *12*, 8611-8632.

(10) Baustian, K.J.; Wise, M.E.; Jensen, E.J.; Schill, G.P.; Freedman, M.A.; Tolbert, M.A. State Transformations and Ice Nucleation in Amorphous (Semi-)Solid Organic Aerosol. *Atmos. Chem. Phys.* **2013**, *13*, 5615-5628.

(11) Price, H.C.; Mattsson, J.; Zhang, Y.; Bertram, A.K.; Davies, J.F.; Grayson, J.W.; Martin, S.T.; O'Sullivan, D.; Reid, J.P.; Rickards, A.M.J.; et al. Water Diffusion in Atmospherically Relevant □-Pinene Secondary Organic Material. *Chem. Sci.* **2015**, *6*, 4876-4883.

(12) Murray, B. Inhibition of Ice Crystallisation in Highly Viscous Organic Acid Droplets. *Atmos. Chem. Phys.* **2008**, *8*, 5423-5433.

(13) Zobrist, B.; Marcolli, C.; Pedernera, D.A. ; Koop, T. Do Atmospheric Aerosols Form Glasses ? *Atmos. Chem. Phys.* **2008**, *8*, 5221-5244.

(14) Darvas, M.; Picaud, S.; Jedlovszky, P. Water Adsorption Around Oxalic Acid Aggregates: A Molecular Dynamics Simulation of Water Nucleation on Organic Aerosols. *Phys. Chem. Chem. Phys.* **2011**, 13, 19830-19839.

(15) Darvas, M.; Picaud, S.; Jedlovszky, P. Molecular Dynamics Simulations of the Water Adsorption Around Malonic Acid Aerosol Models. *Phys. Chem. Chem. Phys.* **2013**, *15*, 10942-10951.

(16) Vardanega, D.; Picaud, S. Water and Formic Acid Aggregates: A Molecular Dynamics Study. *J. Chem. Phys.* **2014**, *141*, 104701.

(17) Radola, B.; Picaud, S.; Vardanega, D.; Jedlovszky, P. Molecular Dynamics Simulations of the Interaction Between Water Molecules and Aggregates of Acetic or Propionic Acid Molecules. *J. Phys. Chem. B* **2015**, *119*, 15662-15674.

(18) Russel, L.M.; Bahadur, R.; Ziemann, P.J. Identifying Organic Aerosol Sources by Comparing Functional Group Composition in Chamber and Atmospheric Particles. *Proc. Natl. Acad. Sci. U.S.A.* **2011**, *108*, 3516-3521.

(19) Compoint, M.; Toubin, C.; Picaud, S. ; Hoang, P.N.M. ; Girardet, C. Geometry and Dynamics of Formic and Acetic Acids Adsorbed on Ice. *Chem. Phys. Lett.* **2002**, *365*, 1-7.

(20) Picaud, S.; Hoang, P.N.M.; Peybernès, N.; Le Calvé, S.; Mirabel, Ph. Adsorption of Acetic Acid on Ice. Experiments and Molecular Dynamics Simulations. *J. Chem. Phys.* **2005**, *122*, 194707.

(21) Jedlovszky, P.; Hantal, Gy.; Neuróhr, K.; Picaud, S.; Hoang, P. N. M.; von Hessberg, P.; Crowley, J. N. Adsorption Isotherm of Formic Acid on The Surface of Ice, as Seen from Experiments and Grand Canonical Monte Carlo Simulation. *J. Phys. Chem. C* **2008,** *112*, 8976-8987.

(22) Darvas, M.; Picaud, S.; Jedlovszky, P. Molecular Dynamics Simulation of the Adsorption of Oxalic Acid on Ice Surface. *ChemPhysChem.* **2010**, *11*, 3971-3979.

(23) Li, X. ; Hede, T. ; Tu, Y. ; Leck, C. ; Ågren, H. Surface-Active *cis*-Pinonic Acid in Atmospheric Droplets: A Molecular Dynamics Study. *J. Phys. Chem. Lett.* **2010**, *1*, 769-773.

(24) Hede, T. ; Li, X. ; Leck, C.; Tu, Y. ; Ågren, H. Model HULIS Compounds in Nanoaerosol Clusters - Investigations of Surface Tension and Aggregate Formation Using Molecular Dynamics Simulations. *Atmos. Chem. Phys.* **2011**, *11*, 6549-6557.

(25) Ma, X. ; Chakraborty, P. ; Henz, B.J. ; Zachariah, M.R. Molecular Dynamic Simulation of Dicarboxylic Acid Coated Aqueous Aerosol: Structure and Processing of Water Vapor. *Phys. Chem. Chem. Phys.* **2011**, *13*, 9374-9384.

(26) Sun, L. ; Li, X. ; Hede, T. ; Tu,Y. ; Leck, C. ; Ågren, H. Molecular Dynamics Simulations of the Surface Tension and Structure of Salt Solutions and Clusters. *J. Phys. Chem. B* **2012**, *116*, 3198-3204.

(27) Li, X. ; Hede, T. ; Tu, Y. ; Leck, C. ; Ågren, H. Cloud Droplet Activation Mechanism of Amino Acid Aerosol Particles: Insight from Molecular Dynamics Simulations. *Tellus B* **2013**, *65*, 20476.

(28) Sun, L. ; Hede, T. ; Tu, Y. ; Leck, C. ; Ågren, H. Combined Effect of Glycine and Sea Salt on Aerosol Cloud Droplet Activation Predicted by Molecular Dynamics Simulations. *J. Phys. Chem. A* **2013**, *117*, 10746-10752.

(29) Schill, G.; Tolbert, M.A. Depositional Ice Nucleation on Monocarboxylic Acids: Effects of the O:C Ratio. *J. Phys. Chem. A* **2012**, *116*, 6817-6822.

(30) Meng, Z.; Seinfeld, S.H.; Saxena, P. Gas/Aerosol Distribution of Formic and Acetic Acids. *Aerosol Sci. Tech.* **1995**, *23*, 561-578.

(31) Petters, M.D.; Kreidenweis, S.M. A Single Parameter Representation of Hygroscopic Growth and Cloud Condensation Nucleus Activity. *Atmos. Chem. Phys.* **2007**, *7*, 1961-1971.

(32) Abraham, M.J.; van der Spoel, D.; Lindahl, E.; Hess, B. and the GROMACS development team, GROMACS User Manual version 5.0.4, www.gromacs.org (2014)

(33) Bussi, G.; Donadio, D.; Parrinello, M. Canonical Sampling Through Velocity Rescaling. *J. Chem. Phys.* **2007**, *126*, 014101.

(34) Jorgensen, W. L.; Maxwell, D. S.; Tirado-Rives, J. Development and Testing of the OPLS All-Atom Force Field on Conformational Energetics and Properties of Organic Liquids. *J. Am. Chem. Soc.* **1996**, *118*, 11225−11236.

(35) Malde, A. K.; Zuo, L.; Breeze, M.; Stroet, M.; Poger, D.; Nair, P. C.; Oostenbrink, C.; Mark, A. E. An Automated Force Field Topology Builder (ATB) and Repository: Version 1.0. J. Chem. Theory Comput. 2011, 7, 4026−4037.

(36) Jedlovszky, P.; Turi, L. A New Five-Site Pair Potential for Formic Acid in Liquid Simulations. *J. Phys. Chem. A* **1997,** *101*, 2662-2665. Corrigendum, *J. Phys. Chem. A* **1999,** *103*, 3796-3796.

(37) Abascal, J.L.F.; Vega, C. A General Purpose Model for the Condensed Phases of Water: TIP4P/2005. *J. Chem. Phys.* **2005**, *123*, 234505.

(38) Mahoney, M. W.; Jorgensen, W. L. A Five-Site Model for Liquid Water and the Reproduction of the Density Anomaly by Rigid, Nonpolarizable Potential Functions. *J. Chem. Phys.* **2000**, *112*, 8910−8922.

(39) Essman, U.; Perera, L.; Berkowitz, M. L.; Darden, T.; Lee, H.; Pedersen, L. G. A Smooth Particle Mesh Ewald Method. *J. Chem. Phys.* **1995,** *103,* 8577-8594.

(40) Hess, B. P-LINCS: A Parallel Linear Constraint Solver for Molecular Simulation. *J. Chem. Theory Comput.* **2008,** *4*, 116-122.

(41) Johnson, C.M.; Tyrode, E.; Baldelli, S.; Rutland, M.W.; Leygraf, C. A Vibrational Sum Frequency Spectroscopy Study of the Liquid-Gas Interface of Acetic Acid-Water Mixtures: 1. Surface Speciation. *J. Phys. Chem. B* **2005**, *109*, 321-328.

(42) Vega, C.; Sanz, E.; Abascal, J. L. F. The Melting Temperature of the Most Common Models of Water. *J. Chem. Phys.* **2005,** *122,* 114507-1-9.

(43) Gadermann, M.; Vollmar, D.; Signorell, R. Infrared Spectroscopy of Acetic Acid and Formic Acid Aerosols: Pure and Compound Acid/Ice Particles. *Phys. Chem. Chem. Phys.* **2007**, *9*, 4535-4544.

(44) Tyrode, E.; Johnson, C.M.; Baldelli, S.; Leygraf, C.; Rutland, M.W.; A Vibrational Sum Frequency Spectroscopy Study of the Liquid-Gas Interface of Acetic Acid-Water Mixtures: 2. Orientation Analysis. *J. Phys. Chem. B* **2005**, *109*, 329-341.

(45) Fedotova, M.V.; Kruchinin, S.E. Hydration of Acetic Acid and Acetate Ion in Water Studied by 1D-RISM Theory. *J. Mol. Liq.* **2011**, *164*, 201-206.

(46) Pruyne, J.G.; Lee, M.T.; Fábri, C.; Beloqui Redondo, A.; Kleibert, A.; Ammann, M.; Brown, M.A.; Krisch, M.J. Liquid-Vapor Interface of Formic Acid Solutions in Salt Water: A Comparison of Macroscopic Surface Tension and Microscopic in Situ X-Ray Photoelectron Spectroscopy Measurements. *J. Phys. Chem. C* **2014**, *118*, 29350-29360.

(47) Lee, M.T.; Orlando, F.; Artiglia, L.; Chen, S.; Ammann, M. Chemical Composition and Properties of the Liquid-Vapor Interface of Aqueous C1 to C4 Monofunctional Acid and Alcohol Solutions. *J. Phys. Chem. A* **2016**, *120*, 9749-9758.

(48) Ma, X. ; Chakraborty, P. ; Henz, B.J. ; Zachariah, M.R. Molecular Dynamic Simulation of Dicarboxylic Acid Coated Aqueous Aerosol: Structure and Processing of Water Vapor. *Phys. Chem. Chem. Phys.* **2011**, *13*, 9374-9384.

(49) Duffey, K.C.; Shih, O.; Wong, N.L.; Drisdell, W.S.; Saykally, R.J.; Cohen, R.C. Evaporation Kinetics of Aqueous Acetic Acid Droplets: Effects of Soluble Organic Aerosol Components on the Mechanism of Water Evaporation. *Phys. Chem. Chem. Phys.* **2013**, *15*, 11634-11639.

(50) Harvey, J.A.; Auerbach, S.M. Simulating Hydrogen-Bond Structure and Dynamics in Glassy Solids Composed of Imidazole Oligomers. *J. Phys. Chem. B* **2014**, *118*, 7609-7617.

(51) Sun, Q.; Harvey, J.A.; Greco, C.; Auerbach, S.M. Molecular Simulations of Hydrogen-Bond Cluster Size and Reorientation Dynamics in Liquid and Glassy Azole Systems. *J. Phys. Chem. B* **2016**, *120*, 10411-10419.

(52) Bateman, A.P.; Bertram, A.K.; Martin, S.T. Hygroscopic Influence on the Semisolid-to-Liquid Transition of Secondary Organic Materials. *J. Phys. Chem. A* **2015**, *119*, 4386-4395.

(53) Slade, J.H.; Knopf, D.A. Multiphase OH Oxidation Kinetics of Organic Aerosol: The Role of Particle Phase State and Relative Humidity. *Geophys. Res. Lett.* **2014**, *41*, 5297-5306.

(54) Slade, J.H.; Shiraiwa, M.; Arangio, A.; Su, H.; Pöschl, U.; Wang, J.; Knopf, D.A. Cloud Droplet Activation Through Oxidation of Organic Aerosol Influenced by Temperature and Particle Phase State. *Geophys. Res. Lett.* **2017**, *44*, 1583-1591.

(55) Lim, C.Y.; Browne, E.C.; Sugrue, R.A.; Kroll, J.H. Rapid Heterogeneous Oxidation of Organic Coatings on Submicron Aerosols. *Geophys. Res. Lett.* **2017**, *44*, 2949-2957

Tables

Table 1. Force Field Parameters of the Different Interaction Models Used in the Simulations for Formic Acid, Acetic Acid, and Water Molecules[a]

Molecule	Site	σ/nm	ε/kJ mol^{-1}	q/e
HCOOH[b]	C	0.3727	0.376	0.44469
	O(C=O)	0.2674	1.214	-0.43236
	O(O—H)	0.3180	0.392	-0.55296
	H(O—H)	0.0994	0.100	0.43331
	H(H—C)	0.0800	0.020	0.10732
CH_3COOH[c]	C(COOH)	0.3750	0.4393	0.52000
	$C(CH_3)$	0.3500	0.2761	-0.18000
	O(C=O)	0.2960	0.8786	-0.44000
	O(O—H)	0.3000	0.7113	-0.53000
	H(O—H)	0.0000	0.0000	0.45000
	H(H—C)	0.2500	0.1255	0.06000
Water[d]	O	0.31589	0.7749	0.0000
	H	0.00000	0.0000	0.55640
	L[e]	0.00000	0.0000	-1.11280

[a] σ, ε and q stand for the Lennard-Jones distance and energy parameters and for the fractional charges, respectively.

[b] Parameters taken from Ref. 36

[c] OPLS-AA force field, taken from Ref. 34

[d] TIP4P/2005 model, Ref. 37

[e] Non-atomic interaction site.

Figures

Figure 1. Equilibrium snapshots of acid-water aggregates for all simulated water-acid ratios at three different temperature values: 150 K (left panel), 225 K (middle panel) and 275 K (right panel). Water molecules are represented by blue color; oxygen, hydrogen and carbon atoms of acid molecules are colored in red, white and green, respectively. Note that these snapshots, taken at the end of the production runs, are not shown on the same scale. Indeed, the aggregates given at the bottom of the figure are in fact much larger than those given at the top because the corresponding systems contain much more water molecules. These snapshots are only provided as illustration of the simulation results.

Figure 2. Cluster size distributions $P(n)$ in the acid-water aggregates for three different water:acid ratios and three temperatures. Distributions are given in black, red, and green colors for acetic acid ($P_{ace}(n)$), formic acid ($P_{for}(n)$), and both acetic and formic acids ($P_{ace+for}(n)$), respectively (see the text). The distribution $P_w(n)$ for the water molecules is given in blue. A value of $P(n)=1$ means that all molecules of the corresponding species form a cluster of n interconnected molecules in the simulation box.

Figure 3. Average cluster size of (a) formic acid and (b) acetic acid clusters formed in the acid-water systems at temperatures ranging from 150 K to 275 K and for various (0:1, 1:1, 2:1, 4:1 and 8:1) water:acid ratios. Lines are only guides to the eye.

Figure 4. Density profiles $\rho(r)$ of (a) acetic acid (black curve), formic acid (red curve) and water (blue curve) molecules and of (b) the carboxyl (yellow curve) and the methyl (green curve) groups of acetic acid molecules, calculated with respect to the aggregate center-of-mass for three different water:acid ratios and three temperature values

Figure 5. Binding energy distributions $P(E_b)$ of mixed formic and acetic acid aggregates interacting with various amounts of water molecules in the simulation box, at three typical temperatures. The binding energy distributions of an acid molecule interacting with all other

acid molecules are given in panel (a) whereas the distributions corresponding to interactions involving the water molecules are given in panel (b). Thus, the binding energy distributions corresponding to the acetic acid – acetic acid, formic acid - formic acid, acetic acid – formic acid, and formic acid – acetic acid interactions are shown on panel (a) by black, red, green and orange color, respectively. The distributions corresponding to the acetic acid – water, formic acid – water, and water – water interactions are shown on panel (b) in purple, magenta and blue color, respectively.

Figure 6. Distributions $P(N_{HB})$ of the number of hydrogen bonds in mixed formic and acetic acid aggregates interacting with various amounts of water molecules at three temperatures. Distribution for H-bonds formed by an acetic acid molecule with other acetic acid molecules, between a formic acid molecule with other formic acid molecules, by an acetic acid molecule with the formic acid molecules, and by a formic acid molecule with the acetic acid molecules are shown by black, red, green and orange colors, respectively, on panel (a). Distributions for H-bonds involving the water molecules are given on panel (b) where purple, magenta, and blue curves correspond to the distributions of the H bonds formed by an acetic acid, a formic acid, and a water molecule with the other water molecules, respectively. Lines are only guides to the eye.

Figure 7. Examples of orientational autocorrelation functions of (a) formic and (b) acetic acid molecules calculated at 150 K (black curve) and 275 K (red curve) and for a 2:1 water:acid ratio.

Figure 1

Radola *et al.*

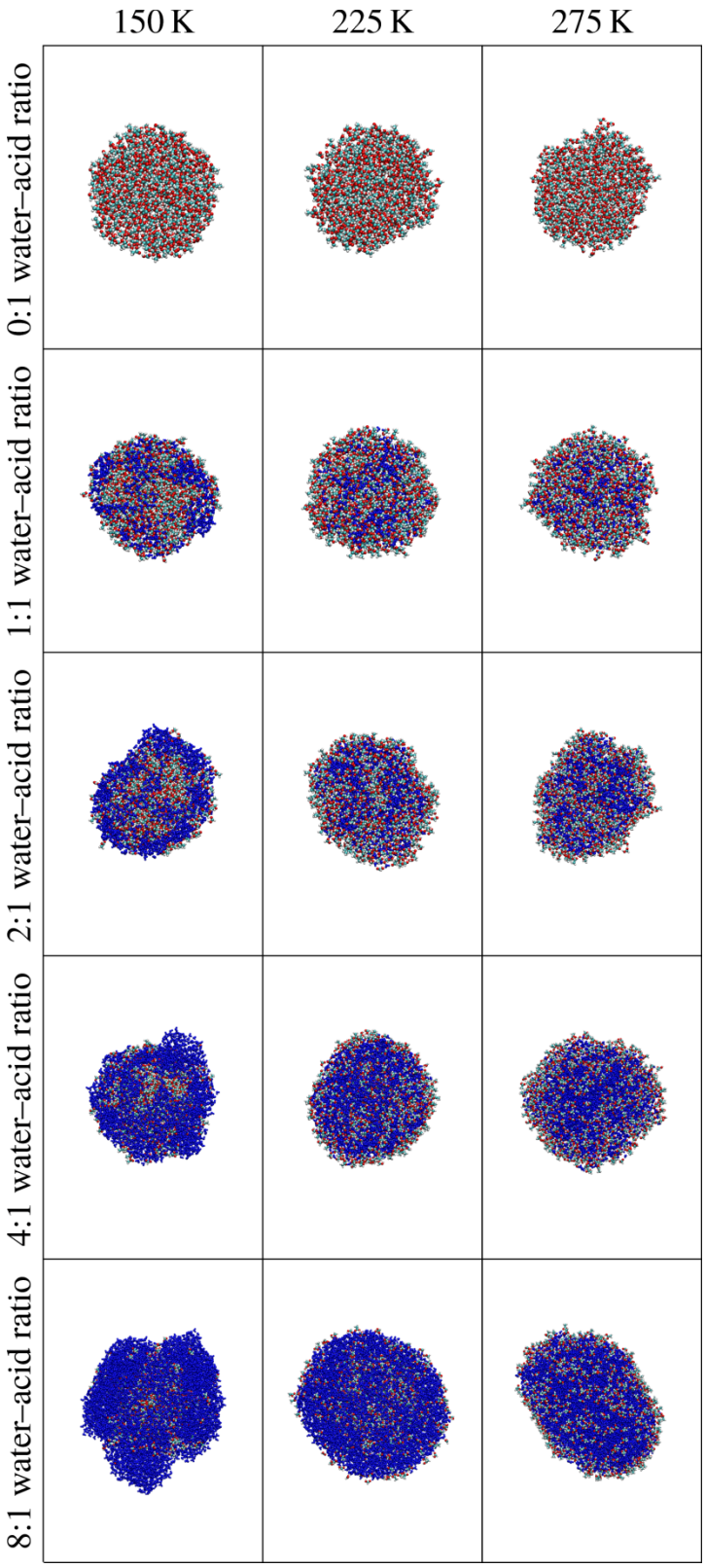

Figure 2

Radola *et al.*

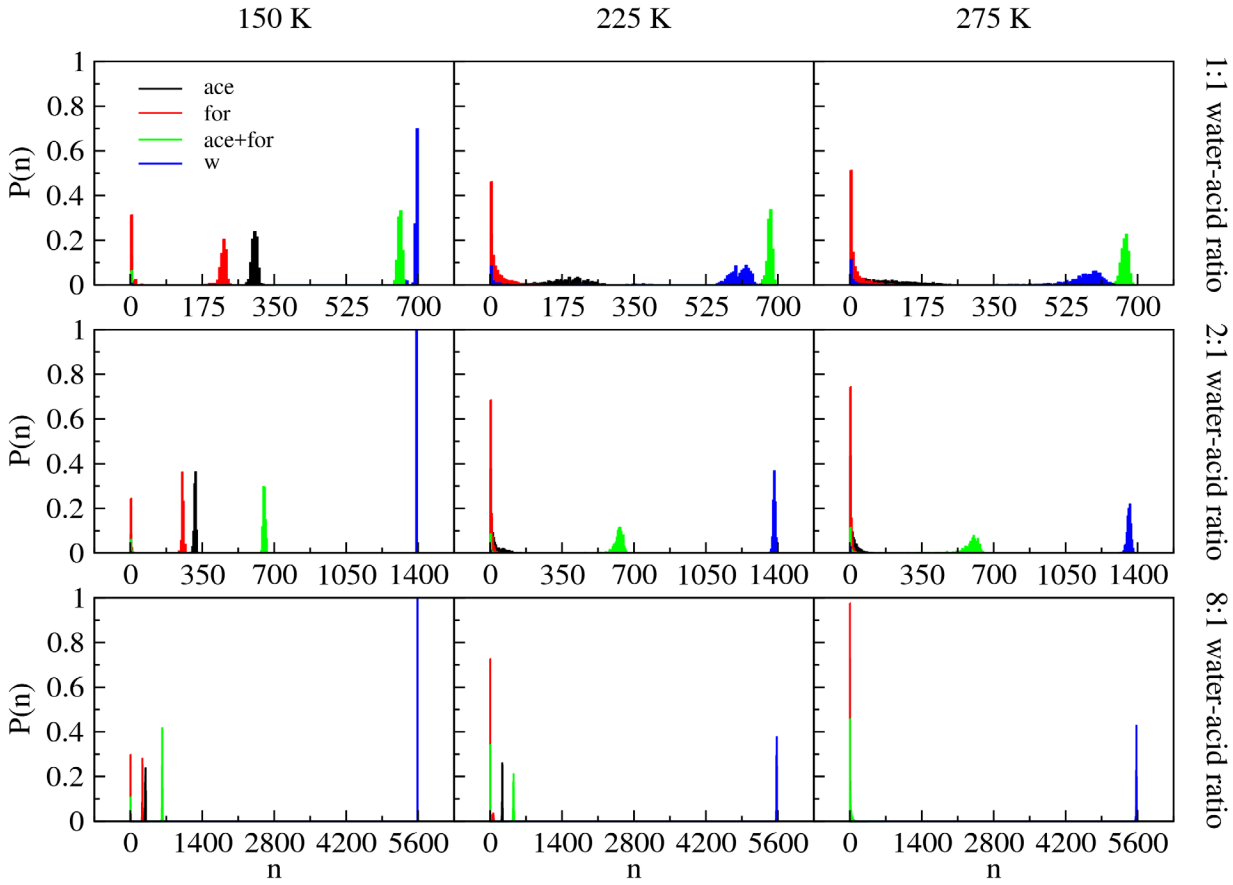

Figure 3

Radola *et al.*

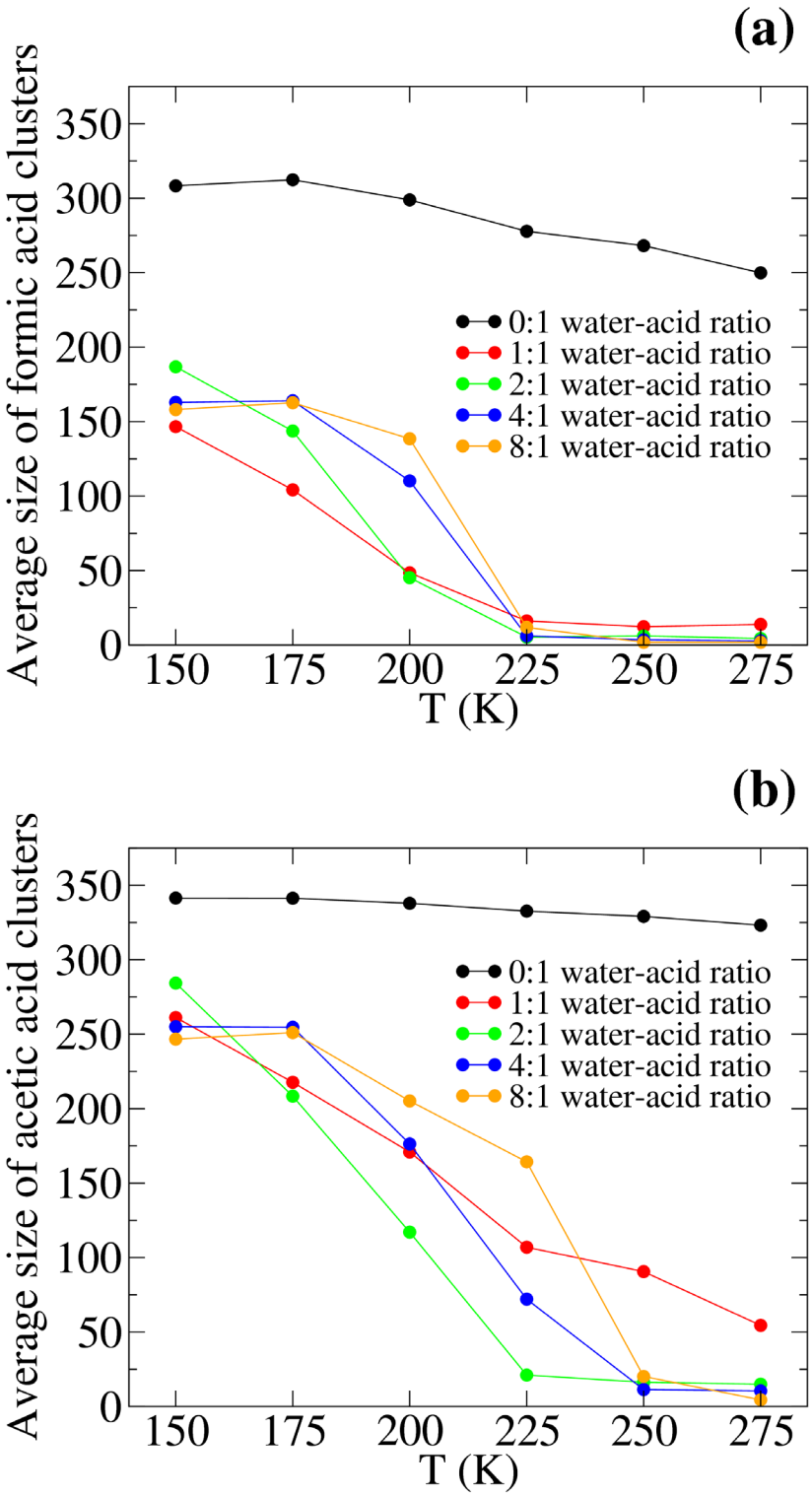

Figure 4a

Radola *et al.*

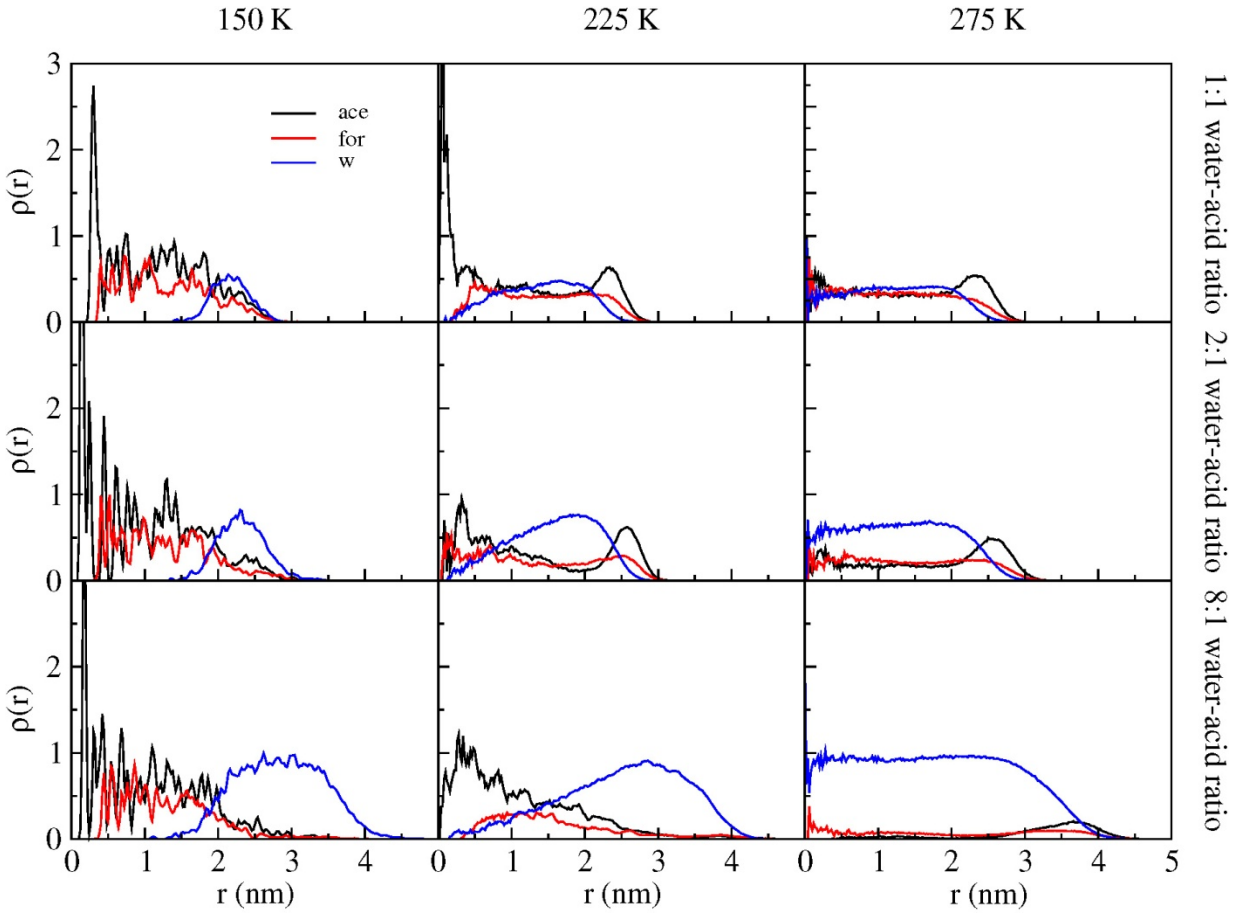

Figure 4b

Radola *et al.*

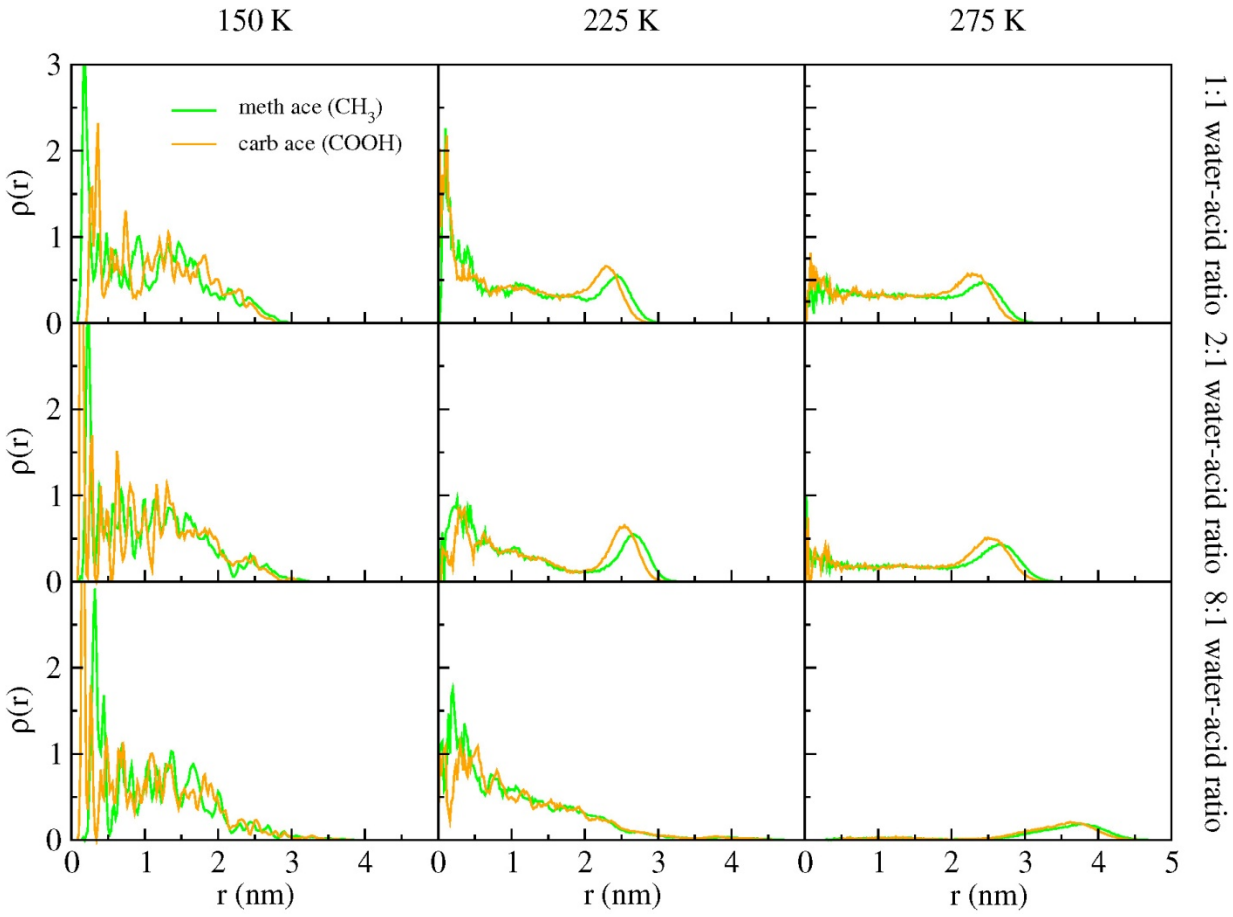

Figure 5a

Radola *et al.*

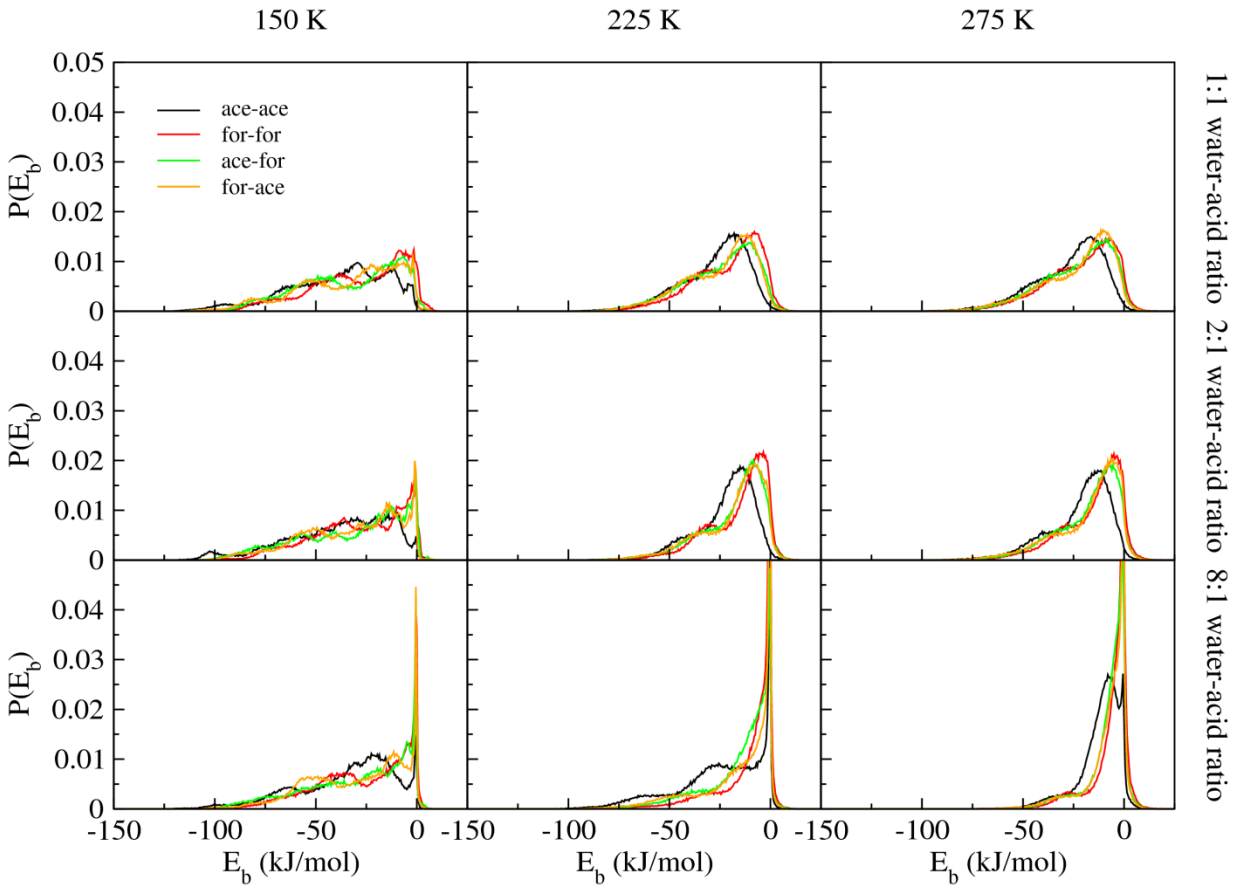

Figure 5b

Radola *et al.*

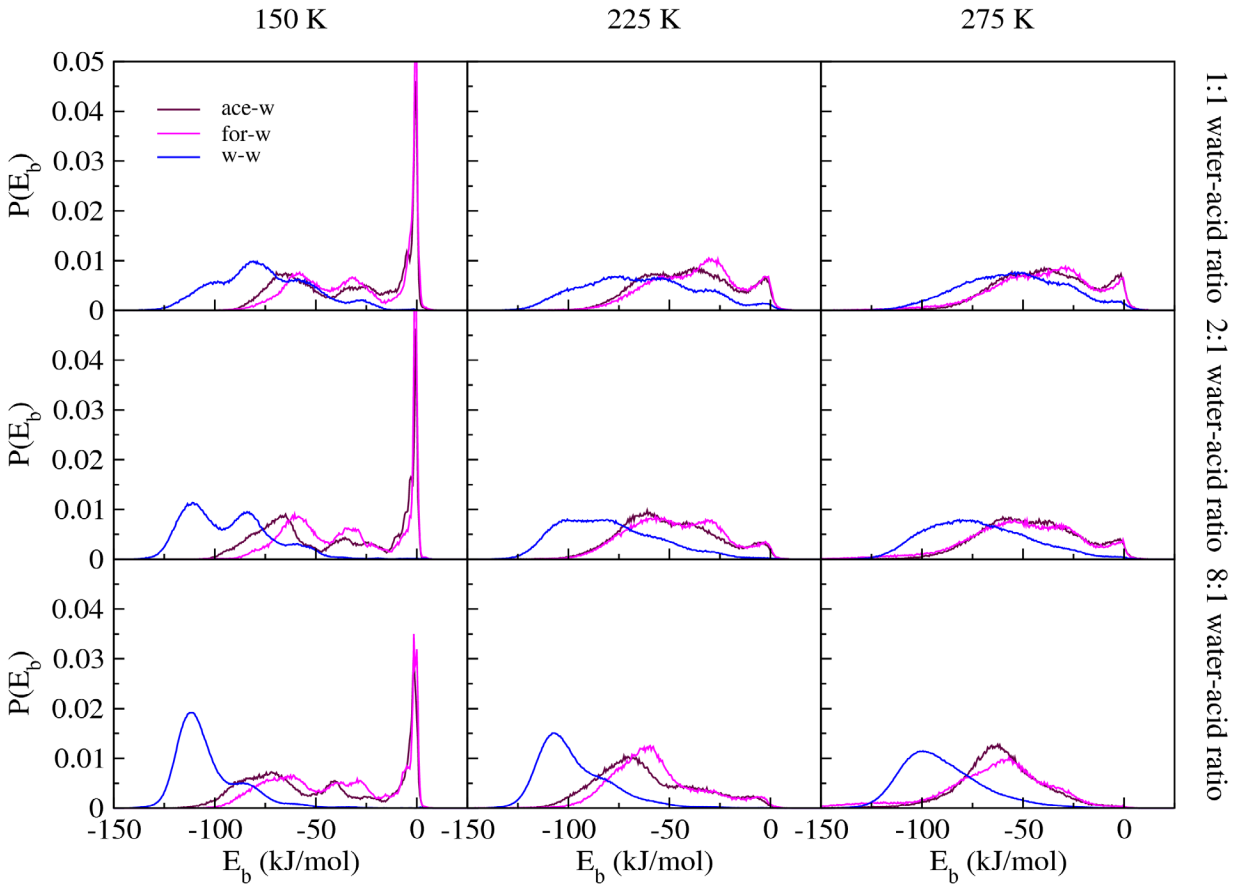

Figure 6a

Radola *et al.*

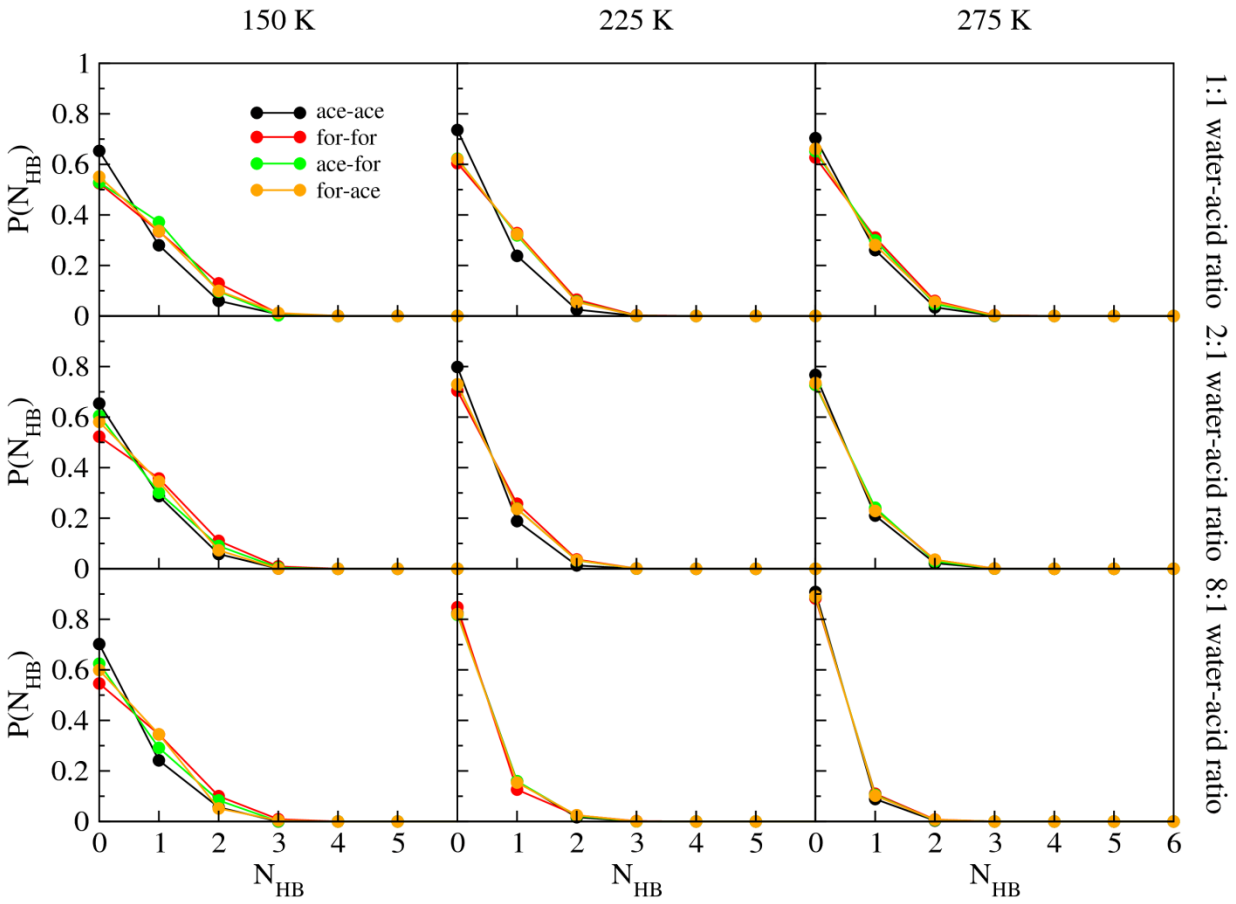

Figure 6b

Radola *et al.*

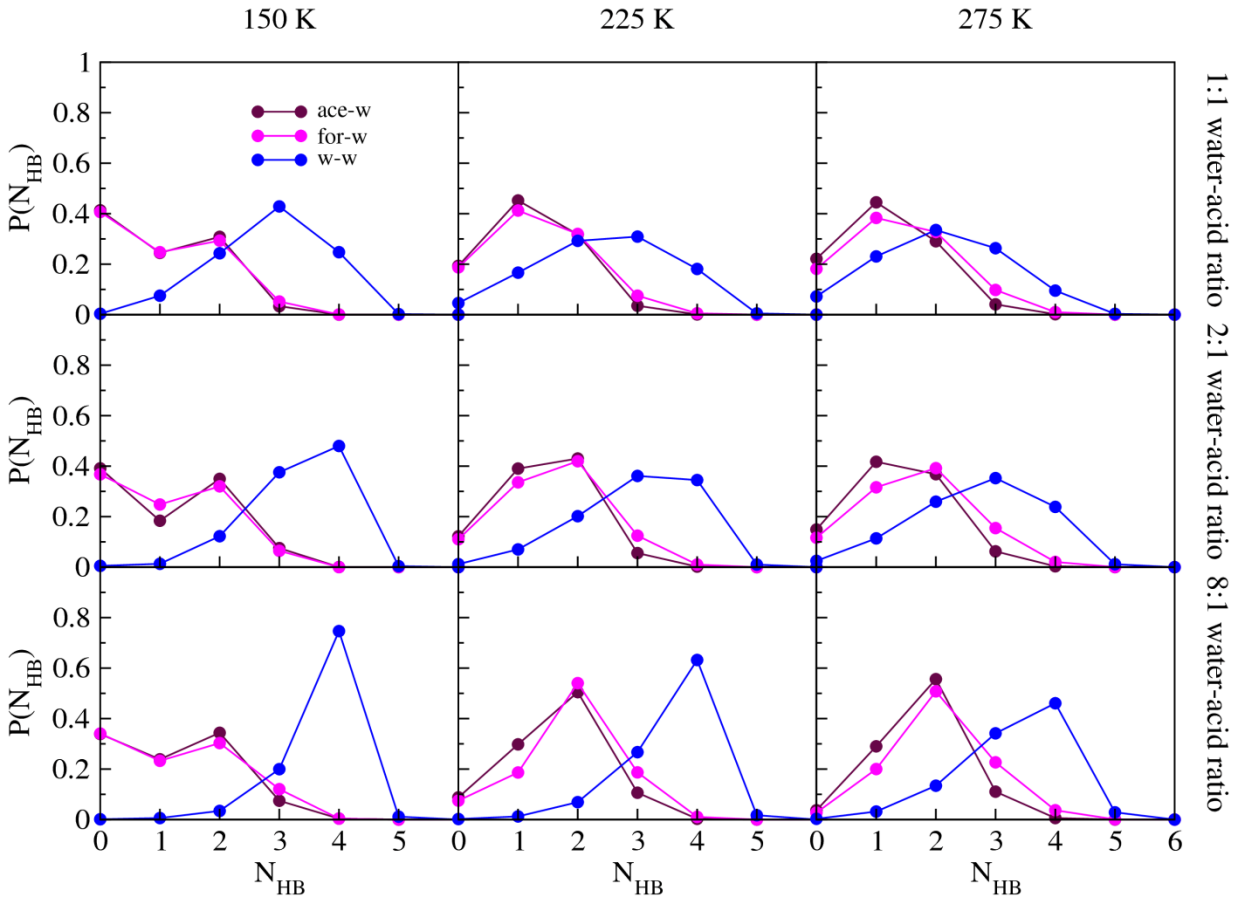

Figure 7

Radola *et al.*

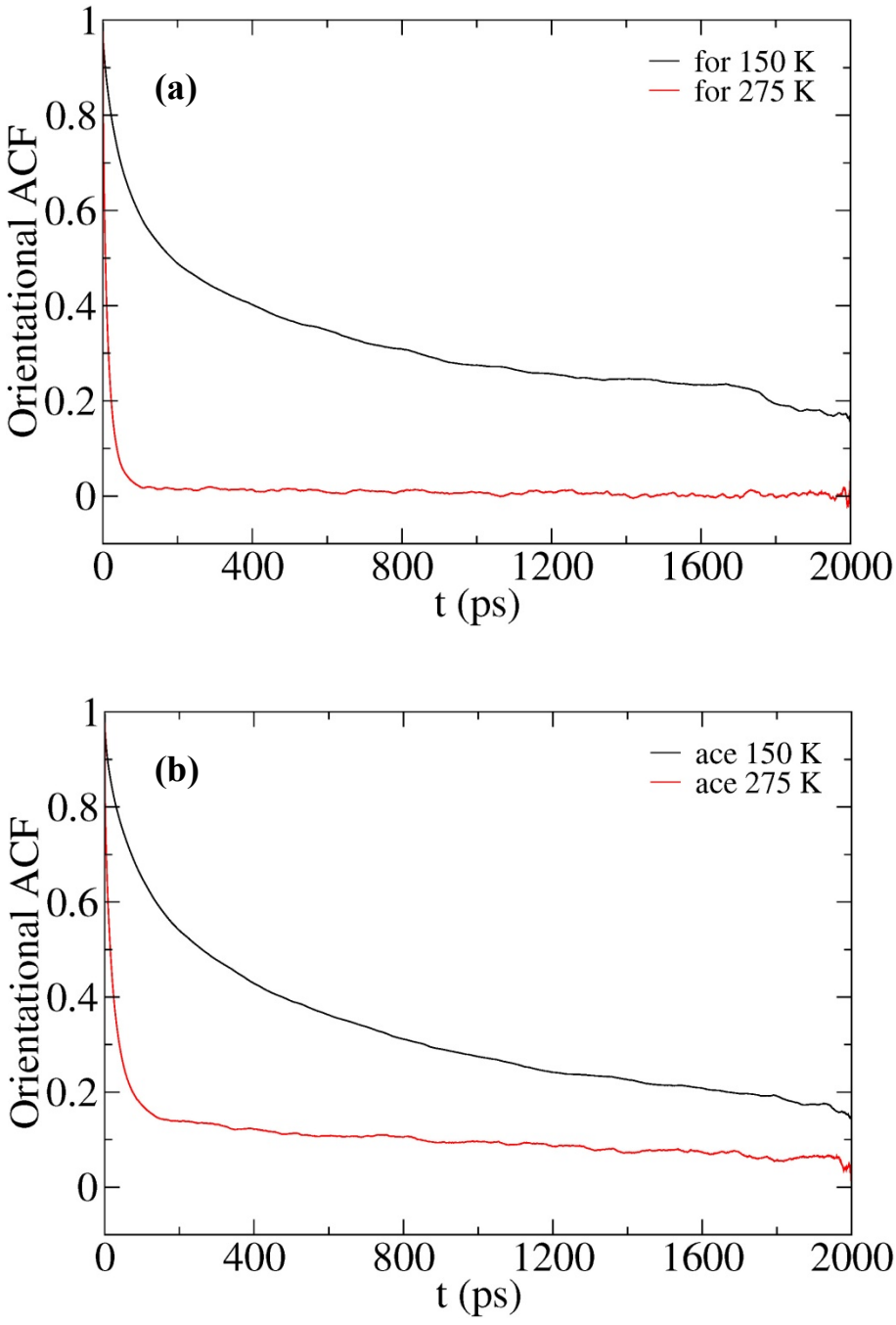

TOC Graphics: